Revista de Climatología

Vol. 21 (2021): 127-145 ISSN 1578-8768

Hydroclimatological extreme events affecting the Daule-Peripa Reservoir (Coast of Ecuador) - Historical dynamics and teleconnections

Dirk Thielen[1], Paolo Ramoni-Perazzi[2], Marco Marquez[1], Jose Quintero[1], Irma Alejandra Soto-Werschitz[3], Wilmer Rojas[1], Kai Thielen[4], Mary L. Puche[1]

[1]*Laboratory of Landscape Ecology and Climate, IVIC, Caracas, 1020-A, Venezuela.*
[2]*Simulation and Modelling Center (CESIMO), University of Los Andes, Mérida, 5101, Venezuela.*
[3]*Departamento de Ecologia e Conservação, Instituto de Ciências Naturais, Universidade Federal de Lavras, Lavras, 37200-900, Minas Gerais, Brazil.*
[4]*Environmental and Resource Management (MSc Study Program), Brandenburg University of Technology Cottbus-Senftenberg, 03046, Cottbus, Germany*

Correspondence to: Dirk Thielen, dirkthielen@gmail.com

(Received: 24-07-2021. Published: 20-09-2021.)

Abstract

An urgent need exists for improved water availability forecasting and monitoring for human activities in response to accelerating climate change. More recently, such planning is under great deal of pressure due to Coronavirus disease 2019 (COVID-19) pandemic and an increasing demand of a reliable provision of clean water for sanitation. The present study analyses spatial and temporal precipitation dynamics as response to very distinctive extreme hydroclimatological events historically affecting the Daule-Peripa Reservoir located in Coast of Ecuador, one of the most climatic vulnerable regions from the Pacific coast of South America, and analyzing the results in terms of foreseeable SST trends. The present study predicts severe and prolonged droughts for the Daule-Peripa Reservoir triggered by a significant warming trend of SSTs occurring in the northern Hemisphere oceanic regions (eg. North Pacific, North Atlantic and the Caribbean Sea). The results provide solid and opportune evidence that can be used at different decision-making levels for identifying, in the context of global climate change scenarios, the most appropriate management practices for the Daule-Peripa Reservoir, information most strategic considering that this reservoir is expected to provide the water related services to a region which population has proven to be at greatest risk from one of the worst pandemics known by humankind in modern times, the COVID-19 pandemic.

Keywords: *Hydroclimatological extreme events, Daule-Peripa Reservoir, Teleconnections, SST warming, Coastal El Niño, Mega El Niño.*

Resumen

Existe una necesidad urgente de mejorar la previsión y el seguimiento de la disponibilidad de agua para las actividades humanas en respuesta al cambio climático acelerado. Más recientemente, dicha planificación se encuentra bajo una gran presión debido a la pandemia de la enfermedad del coronavirus 2019 (COVID-19) y una creciente demanda de un suministro confiable de agua limpia para el saneamiento. El presente estudio analiza la dinámica espacial y temporal de las precipitaciones como respuesta a eventos hidroclimatológicos extremos muy característicos que han afectado históricamente la cuenca del embalse Daule-Peripa (Costa de Ecuador), y analiza los resultados en términos de tendencias previsibles de la Temperatura Superficial de Mar (SST). Este embalse está ubicado en una de las regiones climáticas más vulnerables de la costa del Pacífico de América del Sur. El presente estudio predice sequías severas y prolongadas para la cuenca del embalse Daule-Peripa, generadas por una tendencia de calentamiento significativo de las TSM que ocurren en las regiones oceánicas del hemisferio norte (por ejemplo, Pacífico Norte, Atlántico Norte y Mar Caribe). Los resultados brindan evidencia sólida y oportuna que puede ser utilizada en diferentes niveles de toma de decisiones para identificar, en el contexto de escenarios de cambio climático global, las prácticas de manejo más adecuadas para el Embalse Daule-Peripa, información altamente estratégica considerando que se espera este embalse proporcione los servicios relacionados con el agua a una región cuya población ha demostrado estar en mayor riesgo de una de las peores pandemias conocidas por la humanidad en los tiempos modernos, la pandemia COVID-19.

Palabras clave: *Eventos hidroclimáticos extremos, Reserva del Daule-Peripa Reservoir, Teleconexiones, calentamiento de la SST, Niño Costero, Mega El Niño.*

1. Introduction

An urgent need exists for improved water availability forecasting and monitoring for human activities in response to accelerating climate change. More recently, such planning is under great deal of pressure due to Coronavirus disease 2019 (COVID-19) pandemic and an increasing demand of a reliable provision of clean water for sanitation, prioritizing those regions and populations at greatest risk (Armitage and Nellums, 2020). The Coast of Ecuador has proven to be most vulnerable to this pandemic. Over one third of all COVID-19 cases in continental Ecuador are from this specific region (MSPE, 2021). With an average inflow of 176 m3s-1 (Gelati et al., 2014), an impoundment area of 34,000 ha, and a storage volume over 6.0 km3 (CELEC, 2013), the Daule-Peripa Reservoir is most strategic to Ecuadorian Coast - over 5 million people, that is 35 % of Ecuador´s population, currently rely on drinking water supply from this reservoir, and serves important cities such as Guayaquil (the most populated in Ecuador) and the numerous towns along the Daule/Guayas basin, as well as urban areas from other provinces such as Manabí and Santa Elena. Among other important services also provided by the Daule-Peripa Reservoir to the Coast of Ecuador are: a) Suppling water for irrigation of extended agricultural lands, b) Controlling flooding and mitigate droughts, c) Controlling the salinity and improve navigation on the Guayas and Daule rivers, and d) Generating hydroelectric energy (about 213 MW).

Now, the Coast of Ecuador has a long record of hydroclimatological extreme events, from significant floods to extended droughts (Morán-Tejeda et al., 2016), and capable of affecting water income at the Daule river and Peripa river catchments and condition the reservoir´s service provision. Extreme events are the result from natural climate variability (including phenomena such as El Niño), and natural decadal or multi-decadal variations in the local climate (IPCC, 2012). Their effects are not negligible, and have caused devastating impacts on human's activities and society (Gómez-Martínez et al., 2018). As for El Niño, most economic costs relate to losses of agricultural production and damages to infrastructure, and have been responsible for causing mayor migratory waves (CEPAL, 1998). For instance, over one million Ecuadorians fled the country after affectation on Ecuador´s economy due to El Niño in 72/73 and 82/83 (Bernabé

et al., 2014), as well as in 97/98 (OPS, 2000). As for droughts, Ecuador has suffered significant economic losses over the last decades, mainly in the agricultural and livestock sectors, as well as the hydropower generation (Zambrano-Mera et al., 2018).

El Niño events are large climate disturbances originated by unusual warming of Sea Surface Temperature (SST), from the coasts of Peru and Ecuador to the center of the equatorial Pacific Ocean (Vikas and Dwarakish, 2015), bringing anomalously heavy rainfall to this region (Gelati et al., 2014; Zambrano-Mera et al., 2018). El Niño Southern Oscillation (ENSO) is a coupled ocean–atmosphere phenomenon originating in the tropical Pacific with global impacts. El Niño and La Niña represent the positive (warm) and negative (cool) phases of ENSO, respectively (Sulca et al., 2017). The Oceanic Niño Index (ONI) is NOAA's primary indicator for monitoring ENSO. The ONI tracks the running 3-month average SST in the east-central tropical Pacific between 120°-170° W, specifically the Niño 3.4 region. El Niño occurs when the anomalies exceed +0.5 °C for at least five consecutive months, and it is considered a mega-El Niño when SST anomalies reach +2.0 °C for several months. Three mega-El Niño events have been identified since 1951 (Chen et al., 2017): mega-El Niño of 1982/1983 (mega-EN82/83), 1997/1998 (mega-EN97/98) and 2015/2016 (mega-EN15/16).

Besides El Niño (and mega-El Niño) events, the Coast of Ecuador is also affected by a more local type of hydroclimatological event: The Coastal El Niño. The Coastal El Niño is a very rare and unique event which develops differently from either central or eastern (Pacific) El Niño. According to Hu et al. (2019), a Coastal El Niño develops rather fast and unexpectedly from the warming of SST specific to far eastern tropical Pacific. Until recently, only two of such events were reported - 1891 and 1925 (Takahashi and Martinez, 2017). But early 2017, sea waters off Peru and Ecuador´s coast experienced a rapid, marked warming, causing torrential rains along the west coast of South America (Garreaud, 2018). The Coastal El Niño from early 2017 (hereafter coast-EN17) has been the strongest on record and caused torrential rains along the west coast of tropical South America, with hundreds of fatalities and significant economic losses in Peru and Ecuador. Unlike any historical central or eastern (Pacific) El Niño events, coast-EN17 was not anticipated by climate forecasting centers and left local authorities totally unprepared regarding floods and landslides generated by persistent heavy rains (Ramírez and Briones, 2017; Garreaud, 2018). While recent attention has been brought to the concept of ENSO diversity (Newman et al., 2011; Johnson, 2013; Capotondi et al., 2015; Vikas and Dwarakish, 2015; Sulca et al., 2017; Wang et al., 2017), the Coastal El Niño represents another facet of ENSO that requires further study in terms of its mechanisms and predictability (Takahashi et al., 2018), as well as its potential effects on spatial-temporal dynamics of precipitation anomalies (Schuckmann et al., 2019).

A drought is a natural phenomenon that affects humans much more severely than any other natural events (FAO, 2013). Despite this, drought studies for the Ecuador are very scarce (Campozano et al., 2020). As for the Coast of Ecuador, Vicente-Serrano et al. (2017) state that these dry extreme events can be explained through teleconnections, not only with the tropical Pacific (Niño regions), but with SST dynamics from other oceanic regions, such as northern Pacific and the Atlantic Ocean. There has been an historical human need, exacerbated now by the COVID-19 pandemic, to assertively and fully evaluate, in the context of global climate change and global processes, the effects of most important historical hydroclimatological events capable of generating important spatial-temporal affections, not only in ecosystem functioning, but in the resilience of human activities that rely on local ecosystem services, as well as improving the means forecasting capabilities of such events (Guenni et al., 2016; Tobar and Wyseure, 2017; Thielen et al., 2020).

Regarding aforementioned urge, the present study analyses spatial and temporal precipitation dynamics as response to very distinctive extreme hydroclimatological events historically affecting the Daule-Peripa Reservoir, and analyzing results in terms of foreseeable SST trends. The results provide solid and opportune evidence that can be used at different decision-making levels for identifying, in the context of global climate change scenarios, the most appropriate management practices for the Daule-Peripa Reservoir, information most strategic considering that this reservoir not only is located in one of the most climatic vulnerable regions from the Pacific coast of South America, but it is expected to provide the water related services to a region which population has proven to be at greatest risk from one of the worst pandemics known by humankind in modern times, the COVID-19.

2. Material and Methods

2.1. Study Area

The study area was defined as the 4,542 km2 encompassing the upper part of the Daule river, as well as the entire catchment of the Peripa river, both located at the Coast region of Ecuador, hereafter referred as the Daule-Peripa Reservoir (Fig. 1). The delineation of the Daule-Peripa Reservoir was performed by GIS software from Pfafstetter Level 9 catchments shapefiles provided by https://www.hydrosheds.org/ (Lehner and Grill, 2013).

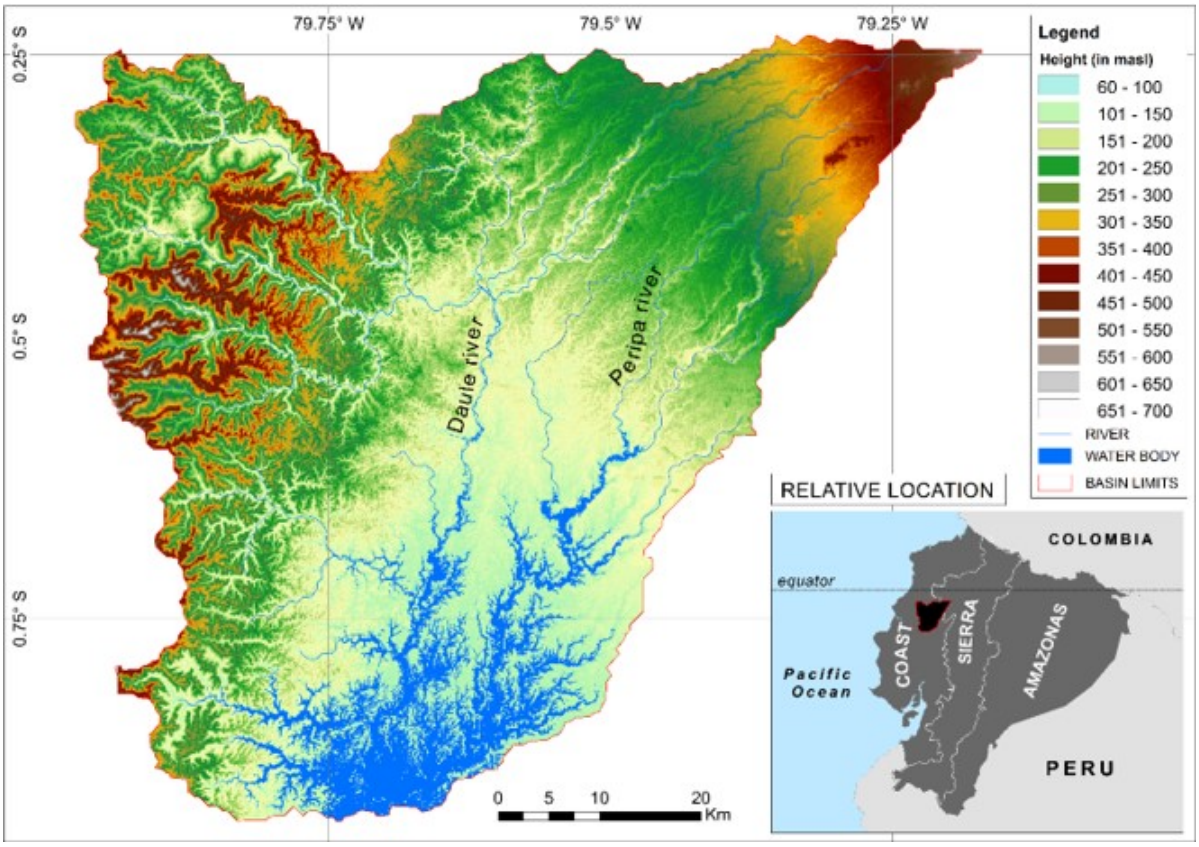

Figure 1: Map of the Daule-Peripa Reservoir at the coast region of Ecuador.

2.2. Data

Precipitation data was obtained from the Climate Hazards group Infrared Precipitation with Stations (CHIRPS V2.0, https://iridl.ldeo.columbia.edu/SOURCES/.UCSB/.CHIRPS/.v2p0/.monthly/.global/). CHIRPS V2.0 is a quasi-global gridded rainfall time series dataset, spanning 50° S-50° N, from 1981 to near-present, 0.05° resolution satellite imagery with in situ station data, with great applications monitoring precipitation extremes (Funk et al., 2015). For the present study, monthly data for the time series Jan-1981/Apr-2020 was obtained from 472 rasters. Monthly and annual mean, as well as some other basic precipitation parameters were obtained by using GIS applications. The monthly mean SST was provided by the NOAA Extended Reconstructed Sea Surface Temperature Version 5 dataset (ERSSTv5), which is a global dataset derived from the International Comprehensive Ocean-Atmosphere Dataset (ICOADS). It is produced on a 2x2-degree grid with spatial completeness enhanced using statistical methods (http://iridl.ldeo.columbia.edu/maproom/Global/Ocean_Temp/Monthly_Temp.html).

2.3. Calculation of monthly Standardized Pluviometric Drought Index (SPDI)

In this study, precipitation spatial-temporal dynamics was analyzed by the Standardized Pluviometric Drought Index (SPDI) developed by Pita (2001). The SPDI is a monthly rainfall index that is based on the calculation of cumulative monthly rainfall anomalies, similar to the well-known Standardized Precipitation Index (SPI) of McKee et al. (1993), more specifically, the 12 month SPI. As in this index, values ranging from +1.0 to +1.5 and +1.5 to +2.0 are associated with moderately humid and very humid episodes, respectively, and values exceeding +2 are representative of extremely humid episodes (see Table 1). Moderately dry, very dry and extremely dry spells are characterized by the same ranges with a negative sign.

Table 1: Categories resulting from SPDI estimation, adapted from McKee et al. (1993).

Range	Category
$\leq$ -2.00	Extremely dry
-1.99 - -1.50	Very dry
-1.49 - -1.00	Moderately dry
-0.99 - 0.99	Near normal
1.00 - 1.49	Moderately humid
1.50 - 1.99	Very humid
$\geq$ 2.00	Extremely humid

The SPDI is calculated as follows:

First stage, Eq. (1):

$$APi = Pi - P_{MED} \tag{1}$$

Where APi is the monthly precipitation anomaly, Pi is the monthly precipitation, and PMED is the median precipitation of the month for the series. As for this study: the series 1981-2010. Second stage, Eq. (2):

$$APAi = \sum APi \tag{2}$$

From i = negative AP to i = positive AP Where APAi is the accumulated precipitation anomaly of the month. Third Stage, Eq. (3):

$$SPDI = (APAi - \overline{APA})/\sigma APA \tag{3}$$

Where $\overline{APA}$ is the average value of accumulated precipitation anomalies of all the months of the series, and σAPA the standard deviation of accumulated precipitation anomalies of all the months of the series.

GIS applications allowed to implement these equations to the 472 aforementioned CHIRPS V2.0 rasters and generate SPDI products such as reservoir-size images of 0.05° resolution, from which monthly zonal values at different space and/or time criteria could be quantified. In the present study, monthly values of SPDI was estimated based on the series 1981-2010. Analysis of monthly SPDI dynamics was performed in the two-year series comprising each main hydroclimatological event, dry or wet. Significance of statistical difference between monthly precipitation and/or SPDI values for any pair of main precipitation event was identified by two-tailed paired t-Test.

2.4. Calculation of correlation of precipitation with the oceanic SSTs

Mean monthly values of SST were estimated by GIS applications for the time series Nov-1981/Apr-2020 and for the following oceanic regions: NIÑO4, NIÑO3.4, NIÑO3, and NIÑO1+2, at the tropical Pacific; PAC-N, at the northern Pacific Ocean; ATL-N, at the northern Atlantic Ocean; and CAR, at the Caribbean Sea (Fig. 2). GIS analytical tools were used to investigate correlations between mean monthly SST and mean monthly precipitation in the study area. Analysis assumed that the observed SST preceded precipitation by lead times of 0 to 6 months. The Pearson correlation coefficient was used to estimate the degree of explained variance (α = 0.01) between the monthly SST and precipitation. A paired, two-tailed t-test was used to assess the significance of statistical differences. Confidence intervals of 99 % were used to identify correlation coefficients (r) ranges. Correlation rasters and associated r values were used to identify the spatial area of oceanic regions with the highest correlation coefficients for observed precipitation (1981–2020) over a range of different lead times. Mann-Kendall tests were applied to determine the significance of the time series trends in the monthly SSTs for each oceanic zone.

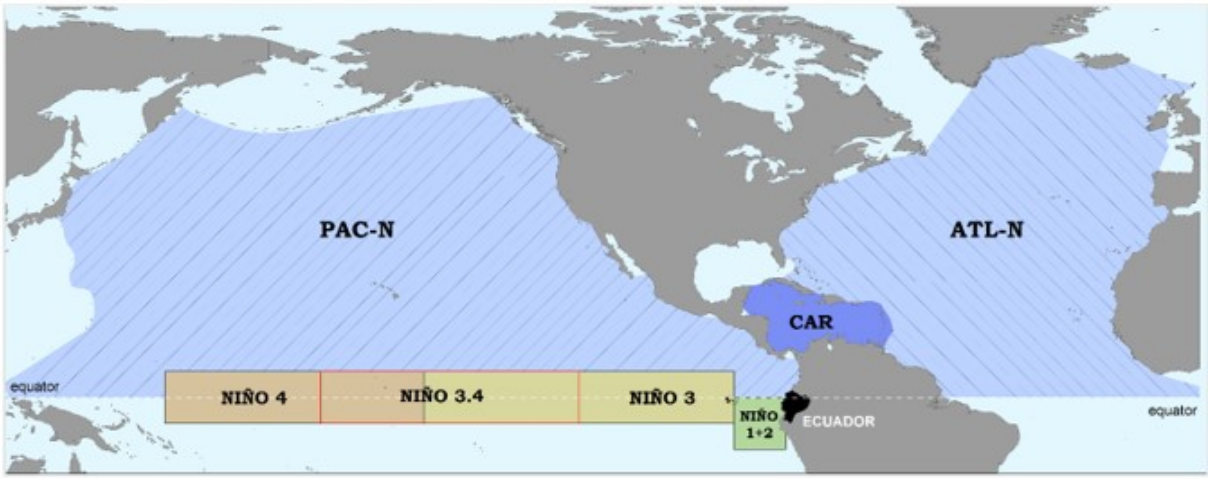

Figure 2: Oceanic regions considered in the present study: NIÑO4, NIÑO3.4, NIÑO3, and NIÑO1+2, at the tropical Pacific; PAC-N, at the northern Pacific Ocean; ATL-N, at the northern Atlantic Ocean; and CAR, at the Caribbean Sea.

3. Results

3.1. Precipitation

Precipitations in the Daule-Peripa Reservoir are highly seasonal – about 74 % of all precipitations occur from January to April (Fig. 3a). For the time series 1981-2010, the mean annual precipitation resulted in 1889 mm, with no evidence of significant trend in the interannual dynamics (Mann-Kendall test, P¿0.05; Fig. 3b). For the 39 years of the series 1981 to 2019, only seven years had annual precipitations above one standard deviation (SD= 608 mm), from which, only one year (1985) was referred to as especially dry, with a precipitation 1.23 SD below from series 1981-2010 annual mean. As for the most humid years, these resulted to be 2017, 1983 and 1997, with positive anomalies of 1.87, 2.91 and 3.03 SD, respectively.

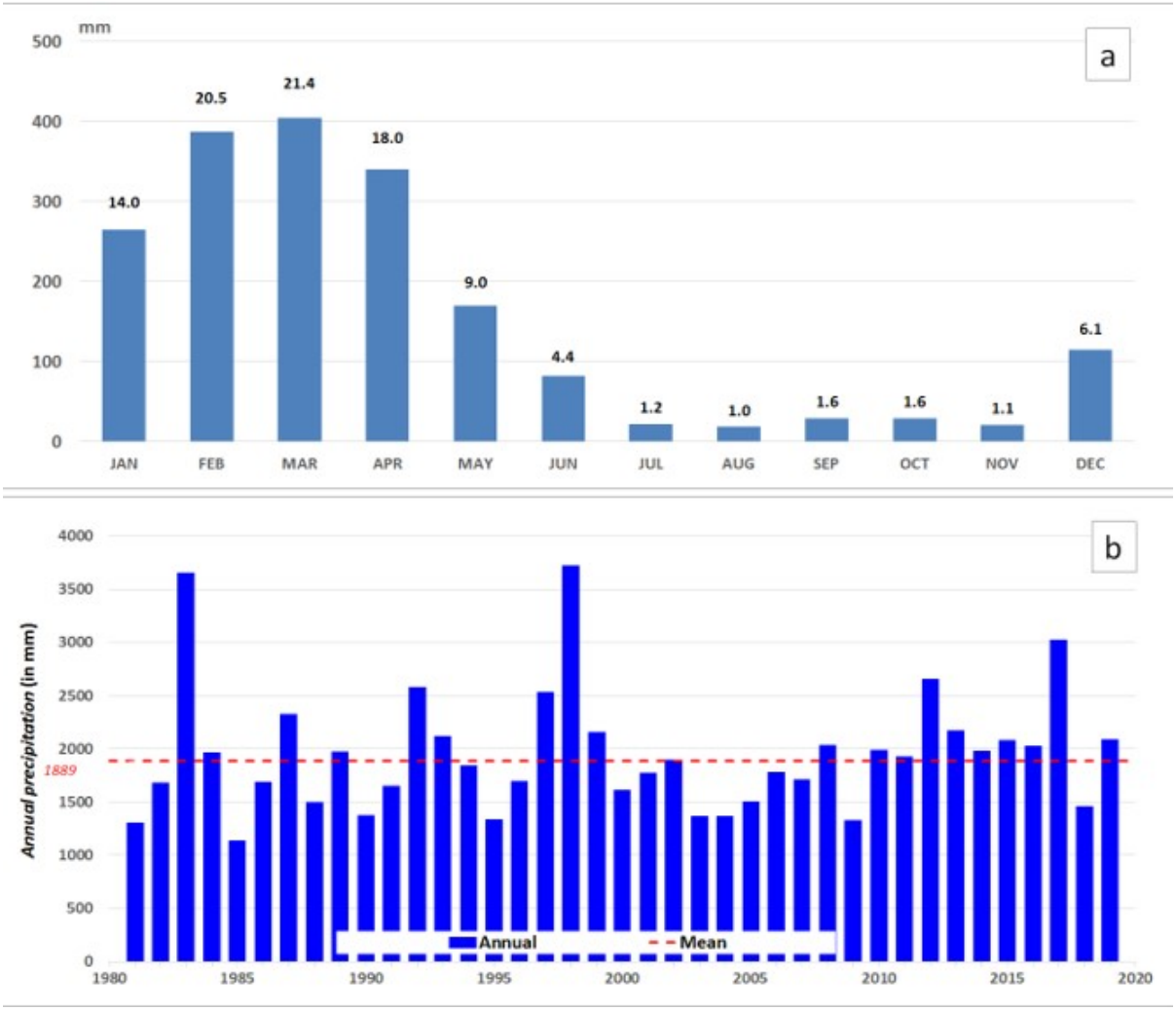

Figure 3: (a) Annual distribution of precipitation at the Daule-Peripa Reservoir, for the series 1981-2010. Labels above bars are referred to corresponding relative (%) values. (b) Interannual distribution of precipitation at the Daule-Peripa Reservoir, western Ecuador.

3.2. Monthly Standardized Precipitation Drought Index (SPDI)

As for the Daule-Peripa Reservoir (see Fig. 4), 79.7 % of the 472 months that comprise the time series January 1981–April 2020 showed an SPDI value Near to Normal, that is -1 ≥SPDI≥ 1 (see Table 1). Here, 7.8 % of the months had a wet condition (SPDI≥ 1.0), from which 3.0 % Moderately Wet (1.0 ≥SPDI< 1.5), 0.6 % Very Wet (1.5 ≥SPDI< 2.0), and 4.2 % Extremely Wet (SPDI≥ 2.0). Likewise, 12.5 % of the months showed a dry condition (SPDI≤ -1), from which mostly were Moderately Dry (12.3 %; -1.0 ≤SPDI> -1.5), and only 0.2 % Very Dry (-1.5 ≤SPDI> -2.0). No Extremely Dry (SPDI≤ -2.0) was registered in Daule-Peripa Reservoir during the 39 years of the series 1981-2019.

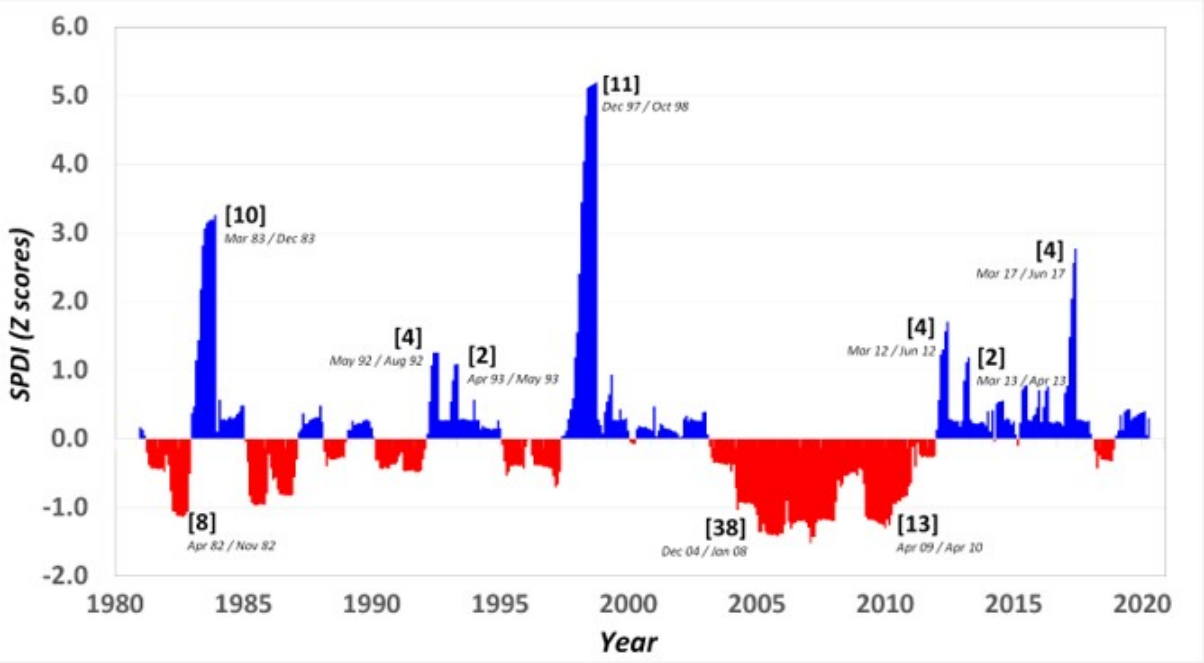

Figure 4: Temporal dynamics in the Standardized Pluviometric Drought Index (SPDI) for the Daule-Peripa Reservoir. Precipitation conditions estimated as SPDI, were interpreted using the classification system from Table 1. The labels are referred to the duration (as consecutive months) of main hydroclimatological events when SPDI reached sustained values above 1.0 or below -1.0.

From Fig. 4 it is also evident that humid episodes are more frequent than dry ones (seven vs. three). Three of these humid hydroclimatological events reached a sustained SPDI category of Extremely Humid (SPDI$\geq$ 2.0) during eight months (May/Dec 83), for 10 months (Feb/Oct 98), and for three months (Apr/Jun 17). As for dry hydroclimatological episodes, although no extreme dry condition (SPDI$\leq$ -2.0) was achieved, two moderately dry spell (1.0 $\geq$SPDI$<$ 1.5) are especially important due to their duration: first, a 38 continuous months' spell (Dec 04/Jan 08), and then a second spell of 13 months (Apr 09/Apr 10). A third, but short-lasting spell (eight months) was obtained from the precipitation analysis. This last dry spell affected precipitations from Apr/Nov 82 generating moderately dry anomalies (1.0 $\geq$SPDI$<$ 1.5) on those months corresponding to 1982´s dry season.

Three global Mega El Niño events are known to have occurred during the series 1981-2020: El Niño 1982/1983 (mega-EN82/83), El Niño 1997/1998 (mega-EN97/98), and El Niño 2015/2016 (mega-EN15/16); as well as one of the strongest Coastal El Niño on record since 1925 (coast-EN17). Figure 5 shows the resulting effects of these important climatological events on precipitations at the Daule-Peripa Reservoir, analyzed in the two-year series comprising each event. Here, results show that, when compared to the historic mean (series 1981-2010), all aforementioned events, but the Mega El Niño 2015/2016 (mega-EN15/16), were capable of generating significant and positive precipitation anomalies in the study area (paired t-Test; P$>$ 0.05). According to Fig. 5a, significant precipitation anomalies, either from Mega El Niño or Coastal El Niño events, are most likely to occur during the first half of Year 2. No anomalies where observed during Year 1, nor Year 3, generated by these extreme humid events. As for Fig. 5b, the analysis of SPDI temporal dynamics, evidence is provided that, for the Daule-Peripa Reservoir, resulting anomalies in monthly precipitation from Mega El Niño or Coastal El Niño events may vary in intensity and duration. Highest SPDI values and for more prolonged time were generated by mega-EN97/98,

followed by mega-EN82/83. In a lesser degree of intensity and duration, coast-EN17 was responsible for generating extreme humid conditions in the study area. The extremely humid condition (SPDI≥ 2.0) generated by these hydroclimatological events ended rather abruptly (Fig. 5b). At a reservoir scale, the mega-EN15/16 did not cause any precipitation anomaly, at any time.

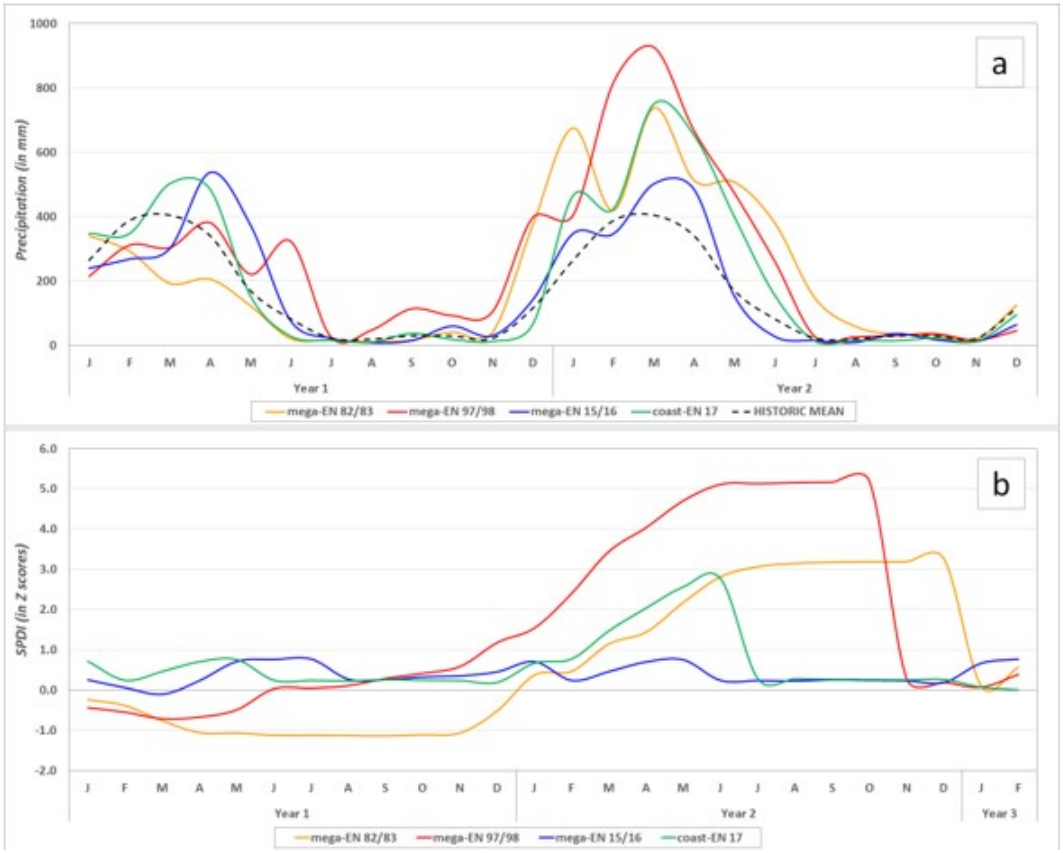

Figure 5: Monthly distribution of (a) Precipitation (in mm) and (b) Standard Pluviometric Drought Index (SPDI, in Z scores) in the Daule-Peripa Reservoir, as response to four climatological extremely humid events referred as the mega-El Niño of 1982/1983 (mega-EN82/83), 1997/1998 (mega-EN97/98) and 2015/2016 (mega-EN15/16), as well as the coastal-El Niño of 2017 (coast-EN17).

Quantification of spatial-temporal dynamics of SPDI values in the Daule-Peripa Reservoir, as response to aforementioned humid hydroclimatological extreme events, is provided in Table 2. From this analysis, it is confirmed that extreme events are capable of generating differentiable responses regarding intensity, duration, as well as extension of precipitation anomalies. For instance, during mega-EN82/83, it was not until almost the end of the first half of Year 2 (May/83) when over 50 % of the Daule-Peripa Reservoir area reached the extremely humid condition (SPDI≥ 2.0), afterwards and for five continuous months (Jun/Oct 83), over 95 % of the study area had SPDI values ≥ 2.0. In the other hand, during mega-EN97/98, such extremely humid condition was reached as early as the second month of Year 2 (Feb/98), and for six continuous months (May/Oct 98), 70 to 90 % of the Reservoir area showed the most extreme anomaly values (SPDI≥ 4.0) for the entire series, and for any of the hydroclimatological events considered in the present study. As for the third Mega El Niño considered in the present study, mega-EN15/16, only 40 % of the study area was affected with anomalous humid condition (SPDI 1.00-1.99), and only for a rather short time (Apr/May 16). Finally, as for coast-EN17, this unusually strong Coastal El Niño and rather local event, affected importantly precipitations at

the Daule-Peripa Reservoir: for four consecutive months (Mar/Jun 17) between 80 and 100 % of the reservoir area had abnormally high SPDI values, where, as for Apr/Jun 17, 61 to 76 % of the area was affected by extremely humid conditions (SPDI≥ 2.0) (Table 2).

Table 2: Spatial-temporal dynamics of SPDI values (see Table 1) in the Daule-Peripa Reservoir as response to humid hydrological extreme events, such as the mega-El Niño of 1982/1983 (mega-EN82/83), 1997/1998 (mega-EN97/98), and 2015/2016 (mega-EN15/16), as well as the coastal-El Niño of 2017 (coast-EN17).

	SPDI		Year 1												Year 2											
	Category	Range	Jan	Feb	Mar	Apr	May	Jun	Jul	Aug	Sep	Oct	Nov	Dec	Jan	Feb	Mar	Apr	May	Jun	Jul	Aug	Sep	Oct	Nov	Dec
mega-EN 82/83	Extremely dry	≤ -2.00	0.0	0.0	0.0	0.0	0.0	0.0	0.0	0.0	0.0	0.0	0.0	0.0	0.0	0.0	0.0	0.0	0.0	0.0	0.0	0.0	0.0	0.0	0.0	0.0
	Very dry	-1.99 - -1.50	0.0	0.0	0.0	4.5	2.0	4.0	4.0	4.0	4.5	3.5	1.5	0.0	0.0	0.0	0.0	0.0	0.0	0.0	0.0	0.0	0.0	0.0	0.0	0.0
	Moderately dry	-1.49 - -1.00	0.0	0.0	10.4	34.3	41.3	43.8	43.8	44.3	44.8	42.3	41.8	7.0	0.0	0.0	0.0	0.0	0.0	0.0	0.0	0.0	0.0	0.0	0.0	0.0
	Near normal	-0.99 - 0.99	100	100	89.6	61.2	56.7	52.2	52.2	51.7	50.7	54.2	56.7	91.5	89.1	92.5	32.8	4.5	0.0	0.0	0.0	0.0	1.5	7.5	64.7	64.7
	Moderately humid	1.00 - 1.49	0.0	0.0	0.0	0.0	0.0	0.0	0.0	0.0	0.0	0.0	0.0	1.5	8.0	7.5	55.7	47.3	0.5	0.0	0.0	0.0	0.0	0.0	0.0	0.0
	Very humid	1.50 - 1.99	0.0	0.0	0.0	0.0	0.0	0.0	0.0	0.0	0.0	0.0	0.0	0.0	3.0	0.0	11.4	43.3	34.8	1.0	0.0	0.0	0.0	0.0	0.0	0.0
	Extremely humid	2.00 - 2.49	0.0	0.0	0.0	0.0	0.0	0.0	0.0	0.0	0.0	0.0	0.0	0.0	0.0	0.0	0.0	5.0	49.3	18.4	3.0	2.5	2.5	2.0	1.5	1.5
	↓	2.50 - 2.99	0.0	0.0	0.0	0.0	0.0	0.0	0.0	0.0	0.0	0.0	0.0	0.0	0.0	0.0	0.0	0.0	15.4	63.2	50.2	42.8	40.8	37.8	17.9	15.9
		3.00 - 3.49	0.0	0.0	0.0	0.0	0.0	0.0	0.0	0.0	0.0	0.0	0.0	0.0	0.0	0.0	0.0	0.0	0.0	15.9	41.3	47.3	46.8	44.8	15.4	16.9
		3.50 - 3.99	0.0	0.0	0.0	0.0	0.0	0.0	0.0	0.0	0.0	0.0	0.0	0.0	0.0	0.0	0.0	0.0	0.0	1.5	5.5	7.5	8.5	8.0	0.5	1.0
		≥ 4.00	0.0	0.0	0.0	0.0	0.0	0.0	0.0	0.0	0.0	0.0	0.0	0.0	0.0	0.0	0.0	0.0	0.0	0.0	0.0	0.0	0.0	0.0	0.0	0.0
mega-EN 97/98	Extremely dry	≤ -2.00	0.0	0.0	0.0	0.0	0.0	0.0	0.0	0.0	0.0	0.0	0.0	0.0	0.0	0.0	0.0	0.0	0.0	0.0	0.0	0.0	0.0	0.0	0.0	0.0
	Very dry	-1.99 - -1.50	0.0	0.0	0.0	0.0	0.0	0.0	0.0	0.0	0.0	0.0	0.0	0.0	0.0	0.0	0.0	0.0	0.0	0.0	0.0	0.0	0.0	0.0	0.0	0.0
	Moderately dry	-1.49 - -1.00	0.0	0.5	6.0	4.0	1.0	0.0	0.0	0.0	0.0	0.0	0.0	0.0	0.0	0.0	0.0	0.0	0.0	0.0	0.0	0.0	0.0	0.0	0.0	0.0
	Near normal	-0.99 - 0.99	100	99.5	94.0	96.0	99.0	96.0	95.5	94.0	89.6	81.6	77.1	44.3	29.4	0.0	0.0	0.0	0.0	0.0	10.9	10.9	26.9	26.9	83.1	100
	Moderately humid	1.00 - 1.49	0.0	0.0	0.0	0.0	0.0	4.0	4.5	6.0	7.5	12.4	14.9	30.8	26.9	2.5	0.0	0.0	0.0	0.0	0.0	0.0	0.0	0.0	0.0	0.0
	Very humid	1.50 - 1.99	0.0	0.0	0.0	0.0	0.0	0.0	0.0	0.0	3.0	5.5	6.0	17.4	26.4	30.3	0.0	0.0	0.0	0.0	0.0	0.0	0.0	0.0	0.0	0.0
	Extremely humid	2.00 - 2.49	0.0	0.0	0.0	0.0	0.0	0.0	0.0	0.0	0.0	0.5	2.0	5.5	11.9	37.3	0.5	0.0	0.0	0.0	0.0	0.0	0.0	0.0	0.0	0.0
	↓	2.50 - 2.99	0.0	0.0	0.0	0.0	0.0	0.0	0.0	0.0	0.0	0.0	0.0	2.0	5.0	24.4	12.9	1.5	0.0	0.0	0.0	0.0	0.0	0.0	0.0	0.0
		3.00 - 3.49	0.0	0.0	0.0	0.0	0.0	0.0	0.0	0.0	0.0	0.0	0.0	0.0	0.5	5.5	69.7	10.9	0.5	0.0	0.0	0.0	0.0	0.0	0.0	0.0
		3.50 - 3.99	0.0	0.0	0.0	0.0	0.0	0.0	0.0	0.0	0.0	0.0	0.0	0.0	0.0	0.0	16.4	53.2	9.5	2.5	2.0	1.5	1.5	1.5	0.0	0.0
		≥ 4.00	0.0	0.0	0.0	0.0	0.0	0.0	0.0	0.0	0.0	0.0	0.0	0.0	0.0	0.0	0.5	34.3	90.0	97.5	87.1	87.6	71.6	71.6	16.9	0.0
sup-EN 15/16	Extremely dry	≤ -2.00	0.0	0.0	0.0	0.0	0.0	0.0	0.0	0.0	0.0	0.0	0.0	0.0	0.0	0.0	0.0	0.0	0.0	0.0	0.0	0.0	0.0	0.0	0.0	0.0
	Very dry	-1.99 - -1.50	0.0	0.0	0.0	0.0	0.0	0.0	0.0	0.0	0.0	0.0	0.0	0.0	0.0	0.0	0.0	0.0	0.0	0.0	0.0	0.0	0.0	0.0	0.0	0.0
	Moderately dry	-1.49 - -1.00	0.0	0.0	0.0	0.0	0.0	0.0	0.0	0.0	0.0	0.0	0.0	0.0	0.0	0.0	0.0	0.0	0.0	0.0	0.0	0.0	0.0	0.0	0.0	0.0
	Near normal	-0.99 - 0.99	100	100	100	100	67.2	62.2	61.7	100	100	100	100	99.5	89.1	97.5	80.1	56.7	57.7	100	100	100	100	100	100	100
	Moderately humid	1.00 - 1.49	0.0	0.0	0.0	0.0	32.8	37.3	37.8	0.0	0.0	0.0	0.0	0.5	10.9	2.5	19.9	31.8	30.3	0.0	0.0	0.0	0.0	0.0	0.0	0.0
	Very humid	1.50 - 1.99	0.0	0.0	0.0	0.0	0.0	0.5	0.5	0.0	0.0	0.0	0.0	0.0	0.0	0.0	0.0	11.4	11.9	0.0	0.0	0.0	0.0	0.0	0.0	0.0
	Extremely humid	2.00 - 2.49	0.0	0.0	0.0	0.0	0.0	0.0	0.0	0.0	0.0	0.0	0.0	0.0	0.0	0.0	0.0	0.0	0.0	0.0	0.0	0.0	0.0	0.0	0.0	0.0
	↓	2.50 - 2.99	0.0	0.0	0.0	0.0	0.0	0.0	0.0	0.0	0.0	0.0	0.0	0.0	0.0	0.0	0.0	0.0	0.0	0.0	0.0	0.0	0.0	0.0	0.0	0.0
		3.00 - 3.49	0.0	0.0	0.0	0.0	0.0	0.0	0.0	0.0	0.0	0.0	0.0	0.0	0.0	0.0	0.0	0.0	0.0	0.0	0.0	0.0	0.0	0.0	0.0	0.0
		3.50 - 3.99	0.0	0.0	0.0	0.0	0.0	0.0	0.0	0.0	0.0	0.0	0.0	0.0	0.0	0.0	0.0	0.0	0.0	0.0	0.0	0.0	0.0	0.0	0.0	0.0
		≥ 4.00	0.0	0.0	0.0	0.0	0.0	0.0	0.0	0.0	0.0	0.0	0.0	0.0	0.0	0.0	0.0	0.0	0.0	0.0	0.0	0.0	0.0	0.0	0.0	0.0
coast-EN 17	Extremely dry	≤ -2.00	0.0	0.0	0.0	0.0	0.0	0.0	0.0	0.0	0.0	0.0	0.0	0.0	0.0	0.0	0.0	0.0	0.0	0.0	0.0	0.0	0.0	0.0	0.0	0.0
	Very dry	-1.99 - -1.50	0.0	0.0	0.0	0.0	0.0	0.0	0.0	0.0	0.0	0.0	0.0	0.0	0.0	0.0	0.0	0.0	0.0	0.0	0.0	0.0	0.0	0.0	0.0	0.0
	Moderately dry	-1.49 - -1.00	0.0	0.0	0.0	0.0	0.0	0.0	0.0	0.0	0.0	0.0	0.0	0.0	0.0	0.0	0.0	0.0	0.0	0.0	0.0	0.0	0.0	0.0	0.0	0.0
	Near normal	-0.99 - 0.99	89.1	97.5	80.1	56.7	57.7	100	100	100	100	100	100	100	86.6	56.7	20.4	1.5	0.0	0.0	78.1	87.1	89.1	97.5	100	100
	Moderately humid	1.00 - 1.49	10.9	2.5	19.9	31.8	30.3	0.0	0.0	0.0	0.0	0.0	0.0	0.0	13.4	41.8	20.9	24.9	10.0	1.5	0.0	0.0	0.0	0.0	0.0	0.0
	Very humid	1.50 - 1.99	0.0	0.0	0.0	11.4	11.9	0.0	0.0	0.0	0.0	0.0	0.0	0.0	0.0	1.5	41.3	12.4	17.9	22.4	0.0	0.0	0.0	0.0	0.0	0.0
	Extremely humid	2.00 - 2.49	0.0	0.0	0.0	0.0	0.0	0.0	0.0	0.0	0.0	0.0	0.0	0.0	0.0	0.0	17.4	25.4	9.5	9.0	0.0	0.0	0.0	0.0	0.0	0.0
	↓	2.50 - 2.99	0.0	0.0	0.0	0.0	0.0	0.0	0.0	0.0	0.0	0.0	0.0	0.0	0.0	0.0	0.0	31.3	26.4	26.4	7.5	5.5	5.0	0.5	0.0	0.0
		3.00 - 3.49	0.0	0.0	0.0	0.0	0.0	0.0	0.0	0.0	0.0	0.0	0.0	0.0	0.0	0.0	0.0	4.5	22.4	21.4	10.0	5.0	5.0	1.5	0.0	0.0
		3.50 - 3.99	0.0	0.0	0.0	0.0	0.0	0.0	0.0	0.0	0.0	0.0	0.0	0.0	0.0	0.0	0.0	0.0	13.9	15.4	3.5	2.5	1.0	0.5	0.0	0.0
		≥ 4.00	0.0	0.0	0.0	0.0	0.0	0.0	0.0	0.0	0.0	0.0	0.0	0.0	0.0	0.0	0.0	0.0	0.0	4.0	1.0	0.0	0.0	0.0	0.0	0.0

As for hydroclimatological extreme events capable of generating a dry condition occurring during the series 1981-2020 in the Daule-Peripa Reservoir, from Fig. 4, it was evident a prolonged dry event extending from 2004 to 2011 that originated drought pulses of varying intensity and extent. Spatial-temporal dynamics of SPDI values of this extreme dry event is given in Table 3. From Apr/04 04 to Apr/11, that is during 85 months, the dry condition (from moderately to very dry, -1.99 ≤SPDI≤ -1.00) was persistent in the study area, in extension that varied from 2 to 82 % of the Reservoir. This prolonged event can be divided into two very distinguishable dry pulses: A 38-months pulse (Dec 04/Jan 06), with a mean affectation of about 60 % of the study area with a mean SPDI value of 1.3; and a shorter pulse of 13-months (Apr 09/Apr 10), affecting about 50 % of the reservoir. These two dry pulses are separated by a 14-months (Feb 08/Mar 09) lapse with any precipitation anomaly (-1 ≥SPDI≥ 1) in over 90 % of the area. Still, moderately dry and moderately wet conditions (SPDI values) affected the remaining area: 8.7 and 1.3 %, respectively.

Table 3: Spatial-temporal dynamics of SPDI values (see Table 1) in the Daule-Peripa Reservoir as response to a dry and prolonged (2004/2011) hydroclimatological extreme event.

	SPDI		Year 1												Year 2											
	Range	Category	Jan	Feb	Mar	Apr	May	Jun	Jul	Aug	Sep	Oct	Nov	Dec	Jan	Feb	Mar	Apr	May	Jun	Jul	Aug	Sep	Oct	Nov	Dec
2004-2005	Extremely dry	≤ -2.00	0.0	0.0	0.0	0.0	0.0	0.0	0.0	0.0	0.0	0.0	0.0	0.0	0.0	0.0	0.0	0.0	0.0	0.0	0.0	0.0	0.0	0.0	0.0	0.0
	Very dry	-1.99 - -1.50	0.0	0.0	0.0	0.0	0.0	0.0	0.0	0.0	0.0	0.0	0.0	0.0	0.0	3.0	7.0	1.5	3.5	7.5	7.5	7.5	6.0	6.5	8.0	5.0
	Moderately dry	-1.49 - -1.00	0.0	0.0	4.0	15.9	9.0	10.0	10.0	10.0	9.0	10.0	10.9	14.9	30.8	75.1	68.7	53.2	71.6	71.1	71.6	72.6	73.6	74.1	73.6	74.1
	Near normal	-0.99 - 0.99	100	100	96.0	84.1	91.0	90.0	90.0	90.0	91.0	90.0	89.1	85.1	69.2	21.9	24.4	45.3	24.9	21.4	20.9	19.9	20.4	19.4	18.4	20.9
	Moderately humid	1.00 - 1.49	0.0	0.0	0.0	0.0	0.0	0.0	0.0	0.0	0.0	0.0	0.0	0.0	0.0	0.0	0.0	0.0	0.0	0.0	0.0	0.0	0.0	0.0	0.0	0.0
	Very humid	1.50 - 1.99	0.0	0.0	0.0	0.0	0.0	0.0	0.0	0.0	0.0	0.0	0.0	0.0	0.0	0.0	0.0	0.0	0.0	0.0	0.0	0.0	0.0	0.0	0.0	0.0
	Extremely humid	2.00 - 2.49	0.0	0.0	0.0	0.0	0.0	0.0	0.0	0.0	0.0	0.0	0.0	0.0	0.0	0.0	0.0	0.0	0.0	0.0	0.0	0.0	0.0	0.0	0.0	0.0
	↓	2.50 - 2.99	0.0	0.0	0.0	0.0	0.0	0.0	0.0	0.0	0.0	0.0	0.0	0.0	0.0	0.0	0.0	0.0	0.0	0.0	0.0	0.0	0.0	0.0	0.0	0.0
		3.00 - 3.49	0.0	0.0	0.0	0.0	0.0	0.0	0.0	0.0	0.0	0.0	0.0	0.0	0.0	0.0	0.0	0.0	0.0	0.0	0.0	0.0	0.0	0.0	0.0	0.0
		3.50 - 3.99	0.0	0.0	0.0	0.0	0.0	0.0	0.0	0.0	0.0	0.0	0.0	0.0	0.0	0.0	0.0	0.0	0.0	0.0	0.0	0.0	0.0	0.0	0.0	0.0
		≥ 4.00	0.0	0.0	0.0	0.0	0.0	0.0	0.0	0.0	0.0	0.0	0.0	0.0	0.0	0.0	0.0	0.0	0.0	0.0	0.0	0.0	0.0	0.0	0.0	0.0
2006-2007	Extremely dry	≤ -2.00	0.0	0.0	0.0	0.0	0.0	0.0	0.0	0.0	0.0	0.0	0.0	0.0	0.0	0.0	0.0	0.0	0.0	0.0	0.0	0.0	0.0	0.0	0.0	0.0
	Very dry	-1.99 - -1.50	4.5	2.5	0.0	0.0	2.5	0.5	0.0	0.0	0.0	0.0	0.0	0.0	2.0	20.9	16.4	19.4	3.0	2.5	3.0	1.5	2.0	3.0	3.0	3.5
	Moderately dry	-1.49 - -1.00	77.1	55.7	13.4	42.3	62.7	53.7	53.2	47.3	47.8	48.3	46.8	53.7	58.7	61.2	54.2	45.3	47.3	45.3	46.8	45.3	47.8	46.8	46.8	47.3
	Near normal	-0.99 - 0.99	18.4	41.8	86.6	57.7	34.8	45.8	46.8	52.7	52.2	51.7	53.2	46.3	39.3	17.9	29.4	35.3	49.8	52.2	50.2	53.2	50.2	50.2	50.2	49.3
	Moderately humid	1.00 - 1.49	0.0	0.0	0.0	0.0	0.0	0.0	0.0	0.0	0.0	0.0	0.0	0.0	0.0	0.0	0.0	0.0	0.0	0.0	0.0	0.0	0.0	0.0	0.0	0.0
	Very humid	1.50 - 1.99	0.0	0.0	0.0	0.0	0.0	0.0	0.0	0.0	0.0	0.0	0.0	0.0	0.0	0.0	0.0	0.0	0.0	0.0	0.0	0.0	0.0	0.0	0.0	0.0
	Extremely humid	2.00 - 2.49	0.0	0.0	0.0	0.0	0.0	0.0	0.0	0.0	0.0	0.0	0.0	0.0	0.0	0.0	0.0	0.0	0.0	0.0	0.0	0.0	0.0	0.0	0.0	0.0
	↓	2.50 - 2.99	0.0	0.0	0.0	0.0	0.0	0.0	0.0	0.0	0.0	0.0	0.0	0.0	0.0	0.0	0.0	0.0	0.0	0.0	0.0	0.0	0.0	0.0	0.0	0.0
		3.00 - 3.49	0.0	0.0	0.0	0.0	0.0	0.0	0.0	0.0	0.0	0.0	0.0	0.0	0.0	0.0	0.0	0.0	0.0	0.0	0.0	0.0	0.0	0.0	0.0	0.0
		3.50 - 3.99	0.0	0.0	0.0	0.0	0.0	0.0	0.0	0.0	0.0	0.0	0.0	0.0	0.0	0.0	0.0	0.0	0.0	0.0	0.0	0.0	0.0	0.0	0.0	0.0
		≥ 4.00	0.0	0.0	0.0	0.0	0.0	0.0	0.0	0.0	0.0	0.0	0.0	0.0	0.0	0.0	0.0	0.0	0.0	0.0	0.0	0.0	0.0	0.0	0.0	0.0
2008-2009	Extremely dry	≤ -2.00	0.0	0.0	0.0	0.0	0.0	0.0	0.0	0.0	0.0	0.0	0.0	0.0	0.0	0.0	0.0	0.0	0.0	0.0	0.0	0.0	0.0	0.0	0.0	0.0
	Very dry	-1.99 - -1.50	8.0	1.0	0.0	0.0	0.0	0.0	0.0	0.0	0.0	0.0	0.0	0.0	0.0	0.0	0.0	3.5	5.5	5.0	5.5	5.5	7.5	8.0	8.0	10.0
	Moderately dry	-1.49 - -1.00	44.3	31.8	11.9	14.9	12.4	6.0	7.0	5.0	3.0	2.5	3.0	7.5	1.5	4.0	11.9	39.8	42.3	44.8	44.3	44.8	42.8	43.8	43.8	45.3
	Near normal	-0.99 - 0.99	47.8	67.2	84.6	83.6	86.1	91.5	91.5	93.0	94.5	95.0	96.0	92.5	98.5	96.0	88.1	56.7	52.2	50.2	50.2	49.8	49.8	48.3	48.3	44.8
	Moderately humid	1.00 - 1.49	0.0	0.0	3.5	1.5	1.5	2.5	1.5	2.0	2.5	2.5	1.0	0.0	0.0	0.0	0.0	0.0	0.0	0.0	0.0	0.0	0.0	0.0	0.0	0.0
	Very humid	1.50 - 1.99	0.0	0.0	0.0	0.0	0.0	0.0	0.0	0.0	0.0	0.0	0.0	0.0	0.0	0.0	0.0	0.0	0.0	0.0	0.0	0.0	0.0	0.0	0.0	0.0
	Extremely humid	2.00 - 2.49	0.0	0.0	0.0	0.0	0.0	0.0	0.0	0.0	0.0	0.0	0.0	0.0	0.0	0.0	0.0	0.0	0.0	0.0	0.0	0.0	0.0	0.0	0.0	0.0
	↓	2.50 - 2.99	0.0	0.0	0.0	0.0	0.0	0.0	0.0	0.0	0.0	0.0	0.0	0.0	0.0	0.0	0.0	0.0	0.0	0.0	0.0	0.0	0.0	0.0	0.0	0.0
		3.00 - 3.49	0.0	0.0	0.0	0.0	0.0	0.0	0.0	0.0	0.0	0.0	0.0	0.0	0.0	0.0	0.0	0.0	0.0	0.0	0.0	0.0	0.0	0.0	0.0	0.0
		3.50 - 3.99	0.0	0.0	0.0	0.0	0.0	0.0	0.0	0.0	0.0	0.0	0.0	0.0	0.0	0.0	0.0	0.0	0.0	0.0	0.0	0.0	0.0	0.0	0.0	0.0
		≥ 4.00	0.0	0.0	0.0	0.0	0.0	0.0	0.0	0.0	0.0	0.0	0.0	0.0	0.0	0.0	0.0	0.0	0.0	0.0	0.0	0.0	0.0	0.0	0.0	0.0
2010-2011	Extremely dry	≤ -2.00	0.0	0.0	0.0	0.0	0.0	0.0	0.0	0.0	0.0	0.0	0.0	0.0	0.0	0.0	0.0	0.0	0.0	0.0	0.0	0.0	0.0	0.0	0.0	0.0
	Very dry	-1.99 - -1.50	18.9	8.5	20.4	9.0	4.5	5.0	3.5	3.5	2.0	2.0	1.5	0.0	0.0	0.0	0.0	0.0	0.0	0.0	0.0	0.0	0.0	0.0	0.0	0.0
	Moderately dry	-1.49 - -1.00	40.3	40.8	33.3	33.3	27.4	27.9	26.4	26.4	24.9	24.9	24.9	18.9	19.4	2.0	4.0	0.0	2.0	2.5	2.5	2.0	2.5	2.5	2.5	2.0
	Near normal	-0.99 - 0.99	40.8	50.7	46.3	57.7	68.2	67.2	70.1	70.1	73.1	73.1	73.6	81.1	80.6	98.0	96.0	100	98.0	97.5	97.5	98.0	97.5	97.5	97.5	98.0
	Moderately humid	1.00 - 1.49	0.0	0.0	0.0	0.0	0.0	0.0	0.0	0.0	0.0	0.0	0.0	0.0	0.0	0.0	0.0	0.0	0.0	0.0	0.0	0.0	0.0	0.0	0.0	0.0
	Very humid	1.50 - 1.99	0.0	0.0	0.0	0.0	0.0	0.0	0.0	0.0	0.0	0.0	0.0	0.0	0.0	0.0	0.0	0.0	0.0	0.0	0.0	0.0	0.0	0.0	0.0	0.0
	Extremely humid	2.00 - 2.49	0.0	0.0	0.0	0.0	0.0	0.0	0.0	0.0	0.0	0.0	0.0	0.0	0.0	0.0	0.0	0.0	0.0	0.0	0.0	0.0	0.0	0.0	0.0	0.0
	↓	2.50 - 2.99	0.0	0.0	0.0	0.0	0.0	0.0	0.0	0.0	0.0	0.0	0.0	0.0	0.0	0.0	0.0	0.0	0.0	0.0	0.0	0.0	0.0	0.0	0.0	0.0
		3.00 - 3.49	0.0	0.0	0.0	0.0	0.0	0.0	0.0	0.0	0.0	0.0	0.0	0.0	0.0	0.0	0.0	0.0	0.0	0.0	0.0	0.0	0.0	0.0	0.0	0.0
		3.50 - 3.99	0.0	0.0	0.0	0.0	0.0	0.0	0.0	0.0	0.0	0.0	0.0	0.0	0.0	0.0	0.0	0.0	0.0	0.0	0.0	0.0	0.0	0.0	0.0	0.0
		≥ 4.00	0.0	0.0	0.0	0.0	0.0	0.0	0.0	0.0	0.0	0.0	0.0	0.0	0.0	0.0	0.0	0.0	0.0	0.0	0.0	0.0	0.0	0.0	0.0	0.0

3.3. Correlation of precipitation with the oceanic SSTs

Figure 6 shows the Pacific Ocean regions which historical SST showed the highest correlation (Pearson) with precipitation dynamics at the Daule-Peripa Reservoir. The oceanic region NIÑO1+2, showed the strongest (r= 0.85) and most significant (P¡0.001) correlation between the warming of SST and an immediate increase (Lag= 0) in monthly precipitation amounts. As for the other El Niño regions (NIÑO3, NIÑO3.4 and NIÑO4), westward, the correlations between SST and precipitation become weaker and less significant, as would take much longer for a measurable response in rainfall, if any.

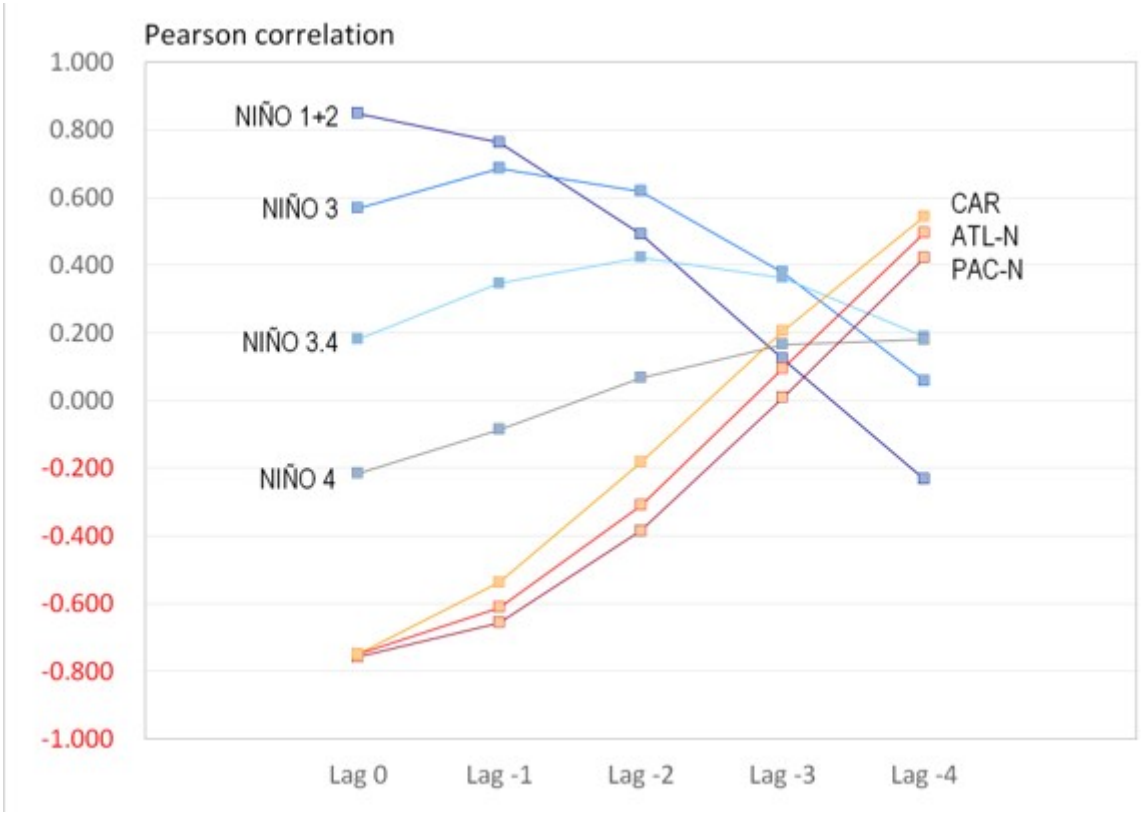

Figure 6: Pearson correlation among different oceanic regions (see Fig. 2) and the precipitations temporal dynamics for the series 1981-2020 at the Daule-Peripa Reservoir.

On the other hand, also from Fig. 6, presence of warm SST at northern Pacific Ocean, as well northern Atlantic Ocean and the Caribbean Sea showed to have a very strong and negative correlations (from -0.77 to -0.74, P¡0.001) with monthly precipitation amounts at the Daule-Peripa Reservoir. From these correlations, rapid responses (Lag= 0) as decrease in monthly precipitation are expected. No significant trend was identified for none of El Niño regions (NIÑO1+2, NIÑO3, NIÑO3.4 and NIÑO4) for the time series 1981-2017. As for the north Pacific Ocean (PAC-N), the northern Atlantic Ocean and the Caribbean Sea did show significant positive trend for the same time series.

4. Discussion

In this study, CHIRPS V2.0 confirmed to be a valuable tool for monitoring hydroclimatological extreme events and contributed to a better understanding of the spatial and temporal variability of monthly rainfall, as demonstrated in other South American regions (Paredes-Trejo et al., 2016; Baez-Villanueva et al., 2018; Rivera et al., 2019; Thielen et al., 2020). Likewise, the application of the SPDI was most appropriate when analyzing temporal and spatial dynamics of precipitation extremes in the Daule-Peripa Reservoir, such as those originated from three distinctive Mega El Niño, the strongest Coastal El Niño on record, and a most prolonged drought. As with the results from the present study, Morán-Tejeda et al. (2016), for the series 1966-2011, did not find a significant trend in precipitation for the Coast of Ecuador. Nevertheless, the precipitation patterns at the Daule-Peripa Reservoir exhibited considerable spatiotemporal dynamics. Overall, the SPDI data showed that about 20 % of the months experienced abnormal precipitation values. Of these, 39 % were related to seven distinctive wet events lasting from

two months up to eleven months. As for the abnormally dry months (61 %), these were related to rather prolonged pulses, lasting from 8 to 38 months. As for the months related to wet events, 54 % reached SPDI values $\geq$ 2.0 (ie. an extremely humid condition); while for the months related to the three dry pulses, although considerably prolonged, 98 % had a (persistently) precipitation anomaly Moderately Dry. It is evident from current results that the major concern about the future occurrence of wet events in the Daule-Peripa Reservoir has to do with - How strong the (extremely wet) precipitation anomaly may become? While for dry hydroclimatological events, major concern would be - How long (persistent) will the (moderately) drought last?

Although the three Mega El Niño (mega-EN82/83, mega-EN97/98 and mega-EN15/16) were the strongest El Niño events on record, their effect on spatial-temporal dynamics of precipitation was distinctive. According to Sanabria et al. (2019), the different sources of moisture contribute to different rainfall patterns between the different sources of moisture contribute to different rainfall patterns between El Niño 1983–1998 and 2016. Regarding this, the present study confirms the NIÑO1+2 as the most important source of precipitation variability for the study area: the warmer the SST at NIÑO1+2 are, the more extremely wet (SPDI $\geq$2.0) the study area becomes. During the Mega El Niño events of 1982/1983 and 1997/1998, as well as in the Coastal El Niño 2017, an important warming of SST at NIÑO1+2 occurred. Such relationship between the magnitude and seasonal distribution of precipitation and the NIÑO1+2 variability was also found by Morán-Tejeda et al. (2016) for the Coast of Ecuador, where forcing is dominant within December–May (Pineda et al., 2013). Observed differences on the effect on spatial-temporal dynamics of precipitation among hydroclimatological extreme events such as meg-EN82/83, meg-EN97/98, meg-EN15/16 and coast-EN17 are mainly due to the time and extend of NIÑO1+2 SST warming.

Results from present study indicate the ENSO region NIÑO1+2 and a lag of zero months are the most reliable predictor of monthly coastal rainfall, contrasting with Guenni et al. (2016) and Zambrano-Mera et al. (2018), who propose the use of ENSO region NIÑO3 with a lagged response of three months. About the use SST of other ENSO regions as predictor, such as NIÑO3.4 and NIÑO4, Bendix et al. (2011) results indicate that these are becoming more unreliable for extreme hydroclimatic situations (floods or droughts) in the southwestern areas of Ecuador. While recent attention has been brought to the concept of ENSO diversity (eg. "central Pacific" vs "eastern Pacific" events; Capotondi et al., 2015), the Coastal El Niño represents another facet of ENSO that requires further study in terms of its mechanisms and predictability (Takahashi et al., 2018). Although Coastal El Niños stand out as a highly uncommon events (Echevin et al., 2018), due to most significant effect generating positive anomalies on precipitation, the present study highlights the necessity not to exclude this event on Daule-Peripa Reservoir long term management practices. A cooling of SST in the NIÑO1+2 region would increase severity and frequency of droughts at the Coast of Ecuador (Vicente-Serrano et al., 2017). Regarding NIÑO1+2 SST trend, Breaker et al. (2016) demonstrated, for the period from 1900 to 2014, a significant positive slope in SST at Ecuador´s coastal waters. But, as shown in results from the present study, such trend is no significant when considering a shorter series (eg. 1981-2017 from this study).

Besides SST at NIÑO1+2, another important driver of variability in the precipitations at the Coast of Ecuador is the Pacific Decadal Oscillation (PDO) (Morán-Tejeda et al., 2016; Vicente-Serrano et al., 2017), a pattern exhibited by the surface waters of the Pacific Ocean north of 20° N, which shifts between warm and cool phases at inter-decadal timescales (Mantua and Hare, 2002). A strong positive correlation was identified between the occurrence dry pulses at Daule-Peripa Reservoir and the warming of northern Pacific Ocean. As results from the present study,

the presence of dry spells in the Coast of Ecuador can be explained by the warming of SST at the north Atlantic Ocean (Haylock et al., 2006; Campozano et al., 2020), as well as the Caribbean Sea. Contrary to SST trend at ENSO regions, a highly significant warming trend of northern Hemisphere sea surface waters has identified in the present study for the series 1981-2017.

5. Conclusion

The present study predicts severe and prolonged droughts for the Daule-Peripa Reservoir triggered by a significant warming trend of SSTs occurring in the northern Hemisphere oceanic regions (eg. North Pacific, North Atlantic and the Caribbean Sea). In developing Countries, extreme climatic events are often challenged by a fragile relationship among the information, climate tools available, and decision-making for inquiring and implementing the best holistic management plans. That is, given the strategic importance and fragility of the study area, all levels of the Ecuadorian Government in coordination with private sectors should develop and implement regional management plans, based on proactive risk management rather than reactive crisis plans to address the various types of impacts resulting from extreme-climate events. Several water management measures should be taken into account, including planning, legislation, public participation, water supply/demand management, cooperation with the international community dealing with water resource management, development of databases, combining water information, training, setting up consciousness and capacity, and motivating the adoption of innovation and technology. Regarding the COVID-19 pandemic, the results provide solid and opportune evidence for identifying, in the context of global climate change scenarios, the most appropriate management practices for the Daule-Peripa Reservoir, information most strategic considering that this reservoir, not only is located in one of the most climatic vulnerable regions from the Pacific coast of South America, but in a region that has proven to be at greatest risk from one of the worst pandemics known by humankind, the COVID-19.

Acknowledgements

Grants from the Organization of American States by the Programa de Alianças para a Educação e a Capacitação (Bolsas Brasil - PAEC OEA-GCUB) were assigned to Paolo Ramoni-Perazzi and Irma Alejandra Soto-Werschitz, allowing their continuous and important participation in the present research. The access to GIS software was provided by Service Unit of Geographical System Information (UniSIG), Ecology Center of the Venezuelan Institute for Scientific Research (IVIC), Caracas, Venezuela.

References

Armitage R, Nellums L (2020): Water, climate change, and COVID-19: prioritising those in water-stressed settings. The Lancet, 10, e175

Baez-Villanueva OM, Zambrano-Bigiarini M, Ribbe L, Nauditt A, Giraldo-Osorio JD, Thinh NX (2018): Temporal and spatial evaluation of satellite rainfall estimates over different regions in Latin-America, *Atmos. Res.*, 213:34-50, doi:10.1016/j.atmosres.2018.05.011

Bendix J, Trachte K, Palacios E, Rollenbeck R, Göttlicher D, Nauss T, Bendix A (2011): El Niño meets La Niña – anomalous rainfall patterns in the "traditional" El Niño region of Southern Ecuador, *Erdkunde*, 65:151-167, doi:10.3112/erdkunde.2011.02.04

Bernabé M, Carreón D, Cerca M, Culqui J, González M, González M, Gutiérrez C, Gutiérrez R, Herrera G, Padilla O, Pauker F, Rodriguez F, Rodríguez G, Salazar R, Toulkeridis T, Vasco C, Zacarías S (2014): Amenazas de origen natural y Gestión de Riesgo en el Ecuador 1. Algunos elementos fundamentales en el manejo de Reducción de Riesgo de Desastres. Editorial ESPE, Quito, Ecuador, 316p

Breaker L, Loor H, Carroll D (2016): Trends in sea surface temperature off the coast of Ecuador and the major processes that contribute to them. *J. Marine Syst.*, 164:151-164, doi:10.1016/j.jmarsys.2016.09.002

Campozano L, Ballari D, Montenegro M, Avilés A (2020): Future meteorological droughts in Ecuador: Decreasing trends and associated spatio-temporal features derived from CMIP5 models. *Front. Earth Sci.*, 8:1-17, doi:10.3389/feart.2020.00017

Capotondi A, Wittenberg A, Newman M, Lorenzo E, Yu J-Y, Braconnot P, Cole J, Dewitte B, Giese B, Guilyardi E, Jin F-F, Karnauskas K, Kirtman B, Lee T, Schneider N, Xue Y, Yeh S-W (2015): Understanding ENSO diversity. *Bulletin of the American Meteorological Society*, 96:921-938, doi:10.1175/BAMS-D-13-00117.1

Corporación Eléctrica del Ecuador - CELEC (2013): Revista 25 Años de la presa Daule-Peripa. CELEC EP-HIDRONACIÓN, 104p.

Comisión Económica para América Latina y El Caribe - CEPAL (1998): Ecuador: Evaluación de los efectos socioeconómicos del fenómeno El Niño 1997-1998, PNUD-CAF, 78p.

Chen L, Li T, Wang B, Wang L (2017): Formation Mechanism for 2015/16 Super El Niño. Sci. Rep., 7, doi:10.1038/s41598-017-02926-3

Echevin V, Colas F, Espinoza-Morriberon D, Vasquez L, Anculle T, Gutierrez D (2018): Forcings and Evolution of the 2017 Coastal El Niño Off Northern Peru and Ecuador. Front. Earth Sci., 5, 1-16, doi:10.3389/fmars.2018.00367

Food and Agriculture Organization – FAO (2013): Paving the Way for National Drought Policies. On line: http://www.fao.org/docrep/018/aq659e/aq659e.pdf, (Last accessed: 18 November 2020).

Funk C, Peterson P, Landsfeld M, Pedreros D, Verdin J, Shukla S, Husak G, Rowland J, Harrison L, Hoell A, Michaelsen J (2015): The climate hazards infrared precipitation with stations—a new environmental record for monitoring extremes. *Sci. Data*, 2:1-21, doi:10.1038/sdata.2015.66

Garreaud R (2018): A plausible atmospheric trigger for the 2017 coastal El Niño. *Int. J. Climatol.*, 38:e1296-e1302, doi:10.1002/joc.5426

Gelati E, Madsen H, Rosbjerg D (2014): Reservoir operation using El Niño forecasts—case study of Daule Peripa and Baba, Ecuador. Hydrolog. Sci. J., 59, 1559-1581, doi:10.1080/02626667.2013.831978

Gómez-Martínez G, Pérez-Martín M, Estrela-Monreal T, Del-Amo P (2018): North Atlantic Oscillation as a cause of the hydrological changes in the Mediterranean (Júcar River, Spain). *Water Resour. Manag.*, 32:2717–2734, doi:10.1007/s11269-018-1954-0

Guenni L, García M, Muñoz Á, Santos J, Cedeño A, Perugachi C, Castillo J (2016): Predicting monthly precipitation along coastal Ecuador: ENSO and transfer function models. *Theor. Appl. Climatol.*, 129:1059-1073, doi:10.1007/s00704-016-1828-4

Haylock M, Peterson T, Alves L, Ambrizzi T, Anunciação Y, Baez J, Barros V, Berlato M, Bidegain M, Coronel G, Corradi V, Garcia V, Grimm A, Karoly D, Marengo J, Marino M, Moncunill D, Nechet D, Quintana J, Rebello E, Rusticucci M, Santos J, Trebejo I, Vincent L (2006): Trends in total and extreme South American rainfall in 1960–2000 and links with Sea Surface Temperature. *J. Clim.*, 19:1490-1512, doi:10.1175/JCLI3695.1

Hu Z-Z, Huang B, Zhu J, Kumar A, Mcphaden M (2019): On the variety of coastal El Niño events. *Clim. Dynam.*, 52: 7537-7552, doi:10.1007/s00382-018-4290-4

Intergovernmental Panel on Climate Change - IPCC (2012): Managing the risks of extreme events and disasters to advance climate change adaptation. Cambridge University Press, 582p.

Johnson N (2013): How many ENSO flavors can we distinguish? *J. Clim.*, 26:4816-4827, doi:10.1175/JCLI-D-12-00649.1

Lehner B, Grill G (2013): Global river hydrography and network routing: baseline data and new approaches to study the world's large river systems. *Hydrol. Process.*, 27:2171–2186, doi:10.1002/hyp.9740

Mantua N, Hare S (2002): The Pacific Decadal Oscillation. *J. Oceanogr.*, 58:33-44.

Mckee T, Doesken N, Kleist J (1993): The relationship of drought frequency and duration to

time scales, 8th Conference on Applied Climatology, Anaheim, California, 179-184.

Morán-Tejeda E, Bazo J, López-Moreno J, Aguilar E, Azorín-Molina C, Sanchez-Lorenzo A, Martínez R, Nieto J, Mejía R, Martín-Hernández N, Vicente-Serrano S (2016): Climate trends and variability in Ecuador (1966–2011). *Int. J. Climatol.*, 36:3839-3855, doi:10.1002/joc.4597

Ministerio de Salud Pública del Ecuador – MSPE (2021): Situación Nacional por COVID-19 - Infografía N°382 – From 29/02/2020 to 15/03/2021.

Newman M, Shin S-I, Alexander M (2011): Natural variation in ENSO flavors. Geophys. Res. Lett., 38, L14705, doi:10.1029/2011GL047658

Organización Panamericana de la Salud - OPS (2000): Crónicas de desastres - Fenómeno El Niño 1997 - 1998. Organización Panamericana de la Salud - OPS. Washington, D.C., 290p.

Paredes-Trejo F, Alves-Barbosa H, Peñaloza-Murillo M, Moreno M, Farias A (2016): Intercomparison of improved satellite rainfall estimation with CHIRPS gridded product and rain gauge data over Venezuela. *Atmósfera*, 29:323-342, doi:10.20937/ATM.2016.29.04.04

Pineda L, Ntegeka V, Willems P (2013): Rainfall variability related to sea surface temperature anomalies in a Pacific–Andean basin into Ecuador and Peru. *Advances in Geosciences*, 33:53-62, doi:10.5194/adgeo-33-53-2013

Pita M (2001): Un nouvel indice de sécheresse pour les domaines méditerranéens. Application au bassin du Guadalquivir (sudouest de l'Espagne). *Publications de l'Association Internationale de Climatologie*, 13:225-233.

Ramírez I, Briones F (2017): Understanding the El Niño Costero of 2017: The definition problem and challenges of climate forecasting and disaster responses. *Int. J. Disaster Risk Sci.*, 8:489-492. doi:10.1007/s13753-017-0151-8

Rivera J, Hinrichs S, Marianetti G (2019): Using CHIRPS Dataset to Assess wet and dry Conditions along the semiarid Central-Western Argentina. Adv. Meteorol., 2019, 8413964, doi:10.1155/2019/8413964

Sanabria J, Carrillo C, Labat D (2019): Unprecedented Rainfall and Moisture Patterns during El Niño 2016 in the Eastern Pacific and Tropical Andes: Northern Peru and Ecuador. Atmosphere, 10, 768, doi:10.3390/atmos10120768

Schuckmann K, Le Traon P-Y, Smith N, Pascual A, Djavidnia S, Gattuso J-P, Grégoire M, Nolan G (2019): The 2017 coastal El Niño - Copernicus Marine Service Ocean State Report. *J. Oper. Oceanogr.*, 12:s1-s123, doi:10.1080/1755876X.2019.1633075

Sulca J, Takahashi K, Espinoza J-C, Vuille M, Lavado-Casimiro W (2017): Impacts of different ENSO flavors and tropical Pacific convection variability (ITCZ, SPCZ) on austral summer rain-

fall in South America, with a focus on Peru. *Int. J. Climatol.*, 38:420-435, doi:10.1002/joc.5185

Takahashi K, Martínez A (2017): The very strong coastal El Niño in 1925 in the far-eastern Pacific. *Climate Dynamics*, 52:7389-7415, doi:10.1007/s00382-017-3702-1

Takahashi K, Karamperidou C, Dewitte B (2018): A theoretical model of strong and moderate El Niño regimes. *Clim. Dynam.*, 52:7477–7493, doi:10.1007/s00382-018-4100-z

Thielen D, Schuchmann K-L, Ramoni-Perazzi P, Marquez M, Rojas W, Quintero J, Isaac-Marques M (2020): Quo vadis Pantanal? Expected precipitation extremes and drought dynamics from changing sea surface temperature. PLoS ONE, 15, e0227437, doi:10.1371/journal.pone.0227437

Tobar V, Wyseure G (2017): Seasonal rainfall patterns classification, relationship to ENSO and rainfall trends in Ecuador. *Int. J. Climatol.*, 38:1808-1819, doi:10.1002/joc.5297

Vicente-Serrano S, Aguilar E, Martínez R, Martín-Hernández N, Azorin-Molina C, Sanchez-Lorenzo A, El-Kenawy A, Tomás-Burguera M, Moran-Tejeda E, López-Moreno J, Revuelto J, Beguería S, Nieto J, Drumond A, Gimeno L, Nieto R (2017): The complex influence of ENSO on droughts in Ecuador. *Clim. Dynam.*, 48:405-427, doi:10.1007/s00382-016-3082-y

Vikas M, Dwarakish G (2015): El Nino: A Review. *International Journal of Earth Sciences and Engineering*, 8:130-137.

Wang X, Tan W, Wang C (2017): A new index for identifying different types of El Niño Modoki events. *Clim. Dynam.*, 50:2753–2765, doi:10.1007/s00382-017-3769-8

Zambrano-Mera Y, Rivadeneira-Vera J, Pérez-Martín M (2018): Linking El Niño Southern Oscillation for early drought detection in tropical climates: The Ecuadorian coast. *Sci. Total Environ.*, 643:193-207, doi:10.1016/j.scitotenv.2018.06.160